Catalysis Today 181 (2012) 14–19

Contents lists available at SciVerse ScienceDirect

Catalysis Today

journal homepage: www.elsevier.com/locate/cattod

Characterization of phenylene-bridged hybrid mesoporous materials incorporating arenetricarbonyl complexes ($–C_6H_4Me(CO)_3–$; Me = Cr, Mo) and their catalytic activities

Takashi Kamegawa, Masakazu Saito, Takahiro Sakai, Masaya Matsuoka*, Masakazu Anpo*

Department of Applied Chemistry, Graduate School of Engineering, Osaka Prefecture University, 1-1 Gakuen-cho, Naka-ku, Sakai, Osaka 599-8531, Japan

ARTICLE INFO

Article history:
Received 23 August 2011
Received in revised form 6 October 2011
Accepted 18 October 2011
Available online 17 November 2011

Keywords:
Inorganic–organic hybrid
Mesoporous
Arenetricarbonyl complex
CVD
Polymerization of phenylacetylene
Dehydrochlorination

ABSTRACT

The successful construction of arenetricarbonyl complexes ($–C_6H_4Me(CO)_3–$; Me = Cr, Mo) was achieved through the direct modification of phenylene ($–C_6H_4–$) moieties of phenylene-bridged hybrid mesoporous materials (HMM-ph) by the simple chemical vapor deposition (CVD) of corresponding metal hexacarbonyls. The pore structure as well as high surface area of HMM-ph were retained even after CVD treatment. It was found that HMM-ph incorporating an arenetricarbonyl molybdenum complex (HMM-phMo$(CO)_3$) exhibited higher catalytic performance for the polymerization of phenylacetylene and dehydrochlorination of 2-chloro-2-methylbutane than HMM-phCr$(CO)_3$. Various spectroscopic investigations revealed that the strength of the chemical bond between the phenylene ligand and metal center of the arenetricarbonyl complexes affects the catalytic performance of HMM-phMe$(CO)_3$ (Me = Cr, Mo) .

1. Introduction

For the past several decades, siliceous mesoporous materials have attracted considerable attention in terms of their potential applications as an adsorbent and catalyst support as well as fillers for chromatography [1–3]. The anchoring of organometallic complexes on their surfaces as well as the incorporation of heteroatoms such as Ti-, Cr- and Mo-atoms within their frameworks are promising ways of designing unique catalysts and photocatalysts [3–10]. On the other hand, recently, the synthesis of mesoporous materials which have bridged organic moieties, i.e., $–CH_2CH_2–$, $–CH{=}CH–$ and $–C_6H_4–$, within their silica frameworks has been achieved by using organosilanes $[(R'O)_3Si–R–Si(OR')_3]$ as a precursor [11–15]. The direct utilization of fascinating framework organic moieties within these inorganic–organic hybrid mesoporous materials (HMM) has been intensively studied in various research fields. For example, light-harvesting and light-emitting systems have been designed by a combination of HMM and organic dyes as guest molecules [16,17]. Solid-acid and solid-base catalysts have also been prepared by the post-synthetic direct modification of framework organic moieties with sulfuric acid ($–SO_3H$) and amino ($–NH_2$) groups, respectively [18–20]. In line with such work, our group has previously reported the direct utilization of organic moieties ($–C_6H_4–$ = phenylene (ph)) within HMM as a “framework ligand”, i.e., the construction of arenetricarbonyl complexes ($–$phMe$(CO)_3–$; Me = Cr, Mo, W) by chemical vapor deposition (CVD) treatment of phenylene-bridged hybrid mesoporous materials (HMM-ph) with corresponding metal hexacarbonyls at elevated temperatures [21,22]. Coelho et al. have also reported the synthesis of the same type of complexes by liquid phase treatment of HMM-ph and their catalytic performances for the epoxidation of olefins [23,24].

In the present study, HMM-ph functionalized by arenetricarbonyl chromium and molybdenum complexes (HMM-phMe$(CO)_3$; Me = Cr, Mo) have been prepared by the CVD method and characterized in detail with various spectroscopic methods. Attention has been focused on a clear determination of the local structure of $–$phMe$(CO)_3–$ (Me = Cr, Mo) complexes by XAFS measurements. Furthermore, the catalytic performance of HMM-phMe$(CO)_3$ (Me = Cr, Mo) has been investigated by the polymerization of phenylacetylene as well as the dehydrochlorination of 2-chloro-2-methylbutane as model reactions in heterogeneous systems.

2. Experimental

2.1. Materials

Octadecyltrimethylammonium chloride, phenylacetylene, and 2-chloro-2-methylbutane were purchased from Tokyo Kasei Kogyo

---

* Corresponding authors. Tel.: +81 72 254 9288; fax: +81 72 254 9910.
E-mail addresses: matsumac@chem.osakafu-u.ac.jp (M. Matsuoka), anpo@osakafu-u.ac.jp (M. Anpo).

0920-5861/$ – see front matter © 2011 Elsevier B.V. All rights reserved.
doi:10.1016/j.cattod.2011.10.019

Co., Ltd. Chromium hexacarbonyl ($Cr(CO)_6$), benzene tricarbonyl chromium ($C_6H_6Cr(CO)_3$), molybdenum hexacarbonyl ($Mo(CO)_6$), and 1,4-bis(triethoxysilyl) benzene were obtained from Aldrich. Dry acetonitrile, dry chloroform, dry tetrahydrofuran and HCl (37%) were obtained from Nacalai Tesque Inc. All chemicals were used without further purification.

2.2. *Synthesis of HMM-ph and HMM-phMe(CO)$_3$ (Me = Cr, Mo)*

HMM-ph was synthesized in accordance with previous literature by Inagaki et al. using 1,4-bis(triethoxysilyl)benzene and octadecyltrimethylammonium chloride [14]. The functionalization of HMM-ph through the reaction of phenylene moieties and $Mo(CO)_6$ was carried out by simple chemical vapor deposition (CVD) treatment at 368 K [21,22]. The obtained sample was denoted as HMM-phMo(CO)$_3$, which incorporates arenetricarbonyl molybdenum complexes (–phMo(CO)$_3$–) within its mesoporous frameworks. HMM-phCr(CO)$_3$ was also prepared by the same process at 398 K using $Cr(CO)_6$ as the CVD source [21,22]. Prior to each CVD treatment, HMM-ph was degassed at 473 K for 2 h. Benzene tricarbonyl molybdenum ($C_6H_6Mo(CO)_3$) as a reference complex was also synthesized by a method reported previously and stored under purified argon atmosphere [25].

2.3. *Characterization of HMM-ph and HMM-phMe(CO)$_3$ (Me = Cr, Mo)*

The X-ray diffraction (XRD) patterns were collected by a Shimadzu XRD-6100 using Cu Kα radiation (λ = 1.5406 Å). The UV–vis spectra were obtained using a Shimadzu UV-2200A spectrophotometer. The FT-IR spectra were recorded with a resolution of 4 cm^{-1} in transmission mode using a JASCO FT-IR 660 Plus apparatus. The Cr K-edge X-ray absorption fine structure (XAFS) spectra were obtained at the BL-12C facility of the Photon Factory at the High-Energy Acceleration Research Organization (KEK) in Tsukuba, Japan. The Mo K-edge XAFS spectra were also recorded at the BL-01B1 facility of SPring-8 at the Japan Synchrotron Radiation Research Institute (JASRI). All spectra were recorded in fluorescence mode with a Si(1 1 1) two-crystal monochromator at 298 K. The extended X-ray absorption fine structure (EXAFS) data were examined using an analysis program (Rigaku REX2000). In order to obtain the radial structure function, Fourier transformations of k^3-weighted EXAFS oscillations in the range of 3–12 Å^{-1} were performed.

2.4. *Polymerization reaction of phenylacetylene*

The polymerization reaction of phenylacetylene (PA) was carried out in a two-necked flask (100 ml) equipped with a reflux condenser and gas adapter connected to an oil bubbler. A mixture of the catalyst (HMM-phMe(CO)$_3$; Me = Cr, Mo, 300 mg) and degassed pure PA (2.0 ml) was heated at 353 K with magnetic stirring for 24 h. After the polymerization reaction, the reaction mixture was added to THF and thoroughly stirred for a washing of the catalyst. The THF-rinsed catalyst was then separated by centrifugation. The product was precipitated in methanol, washed with methanol and then purified by reprecipitation from THF. Only a methanol insoluble polymer was recovered. The polymer yield was determined by gravimetry.

2.5. *Dehydrochlorination reaction of 2-chloro-2-methylbutane*

The dehydrochlorination reaction of 2-chloro-2-methylbutane was carried out in a glass vessel equipped with a vacuum line connector. The catalyst (HMM-phMe(CO)$_3$; Me = Cr, Mo, 90 mg) and degassed 2-chloro-2-methylbutane (0.3 ml) were charged into a glass vessel and then heated at 358 K in an oven. At this temperature, 2-chloro-2-methylbutane and the reaction products exist in gaseous form. After heating for 22 h, a glass vessel was cooled down to 298 K and 1.0 ml of THF was added for the complete recovery and diluting of the substances. Analysis of the substances was performed on a gas chromatograph (Shimadzu GC-14B with a flame ionization detector) equipped with an InertCap® 1 capillary column.

3. Results and discussion

3.1. *Characterization of HMM-ph and HMM-phMe(CO)$_3$ (Me = Cr, Mo)*

Fig. 1 shows the UV–vis absorption spectra of HMM-ph before and after CVD treatment with $Mo(CO)_6$ and chloroform solution of the reference complexes. The peak position of $C_6H_6Mo(CO)_3$ was quite different from that of $Mo(CO)_6$. A typical absorption peak at around 325 nm (Fig. 1(b)) can be assigned to the metal–phenyl intramolecular charge transfer transition of the arenetricarbonyl metal complex [26,27]. In the case of HMM-ph, only the absorption peak due to the π–π^* transition of the framework phenylene moieties was observed at around 275 nm. On the other hand, the UV–vis absorption spectrum of HMM-phMo(CO)$_3$ shows a new intense peak and long-tailed absorption which could not be observed for HMM-ph at around 325 nm and above 350 nm, respectively. This absorption spectrum of HMM-phMo(CO)$_3$ corresponds well to the superimposed absorption of HMM-ph and $C_6H_6Mo(CO)_3$, showing the formation of arenetricarbonyl molybdenum complexes (–phMo(CO)$_3$–) through the reaction of phenylene moieties of HMM-ph and $Mo(CO)_6$ under CVD conditions (Eq. (1)):

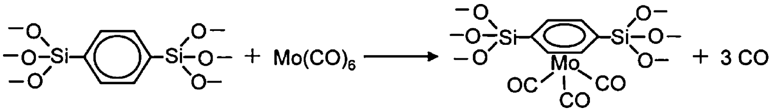

(1)

It should be noted that HMM-phCr(CO)$_3$ also exhibits a typical UV–vis absorption peak at around 320 nm and long-tailed absorption above 350 nm (data not shown) due to the arenetricarbonyl chromium complexes (–phCr(CO)$_3$–) [21,22].

The formation of –phMe(CO)$_3$– (Me = Cr, Mo) complexes within the framework of HMM-ph was also confirmed by FT-IR measurements. As shown in Fig. 2, HMM-phCr(CO)$_3$ and HMM-phMo(CO)$_3$ exhibit typical FT-IR peaks at 1985–1980 and 1940–1840 cm^{-1}, which can be assigned to the a_1 and e vibrational mode of the areneMe(CO)$_3$ (Me = Cr, Mo) complexes, respectively [28–30]. These results clearly indicate the successful construction of –phMe(CO)$_3$– (Me = Cr, Mo) complexes which are coordinated by a phenylene moiety of HMM-ph as a “framework ligand” and confirm the thermal stability of these complexes at temperatures as high as 473 K. The position of the a_1 vibrational mode of HMM-phMo(CO)$_3$ (1984 cm^{-1}) was observed to shift slightly to higher wavenumber regions than that of HMM-phCr(CO)$_3$ (1981 cm^{-1}). It has been reported that the wavenumber of the a_1 vibrational mode of the arenetricarbonyl chromium complexes is closely related to the strength of the metal–arene bond, i.e., the higher the wavenumber of the a_1 vibrational mode, the weaker the strength of the metal–arene bond of the complex [30,31]. The high wavenumber of the a_1 vibrational mode of HMM-phMo(CO)$_3$ indicates that the metal–arene bond of –phMo(CO)$_3$– is weaker than that of –phCr(CO)$_3$–, showing good agreement with previously

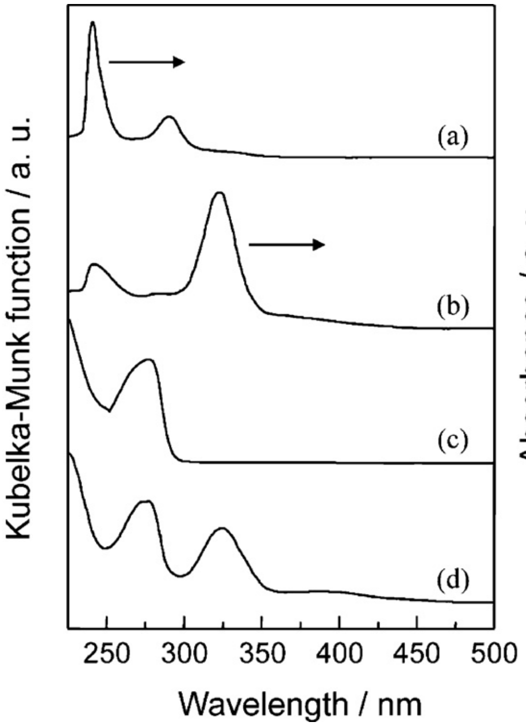

Fig. 1. (a and b) Transmission and (c and d) diffuse reflectance UV–vis spectra of (a) $Mo(CO)_6$ in chloroform, (b) $C_6H_6Mo(CO)_3$ in chloroform, (c) HMM-ph, and (d) HMM-phMo$(CO)_3$.

reported trends showing that the metal–arene bond is weaker for areneMo$(CO)_3$ than areneCr$(CO)_3$ [32].

Moreover, it was also found that these FT-IR peaks completely disappeared after evacuation at 573 K for 1 h by the decomposition of (–phMe$(CO)_3$–; Me = Cr, Mo). CO desorption analysis from HMM-phMe$(CO)_3$ also revealed that the CO desorbed from the complexes above 523 K under vacuum. During this CO desorption process, the sample color of HMM-phMe$(CO)_3$ gradually changed from pale yellow to gray due to the formation of corresponding metal clusters.

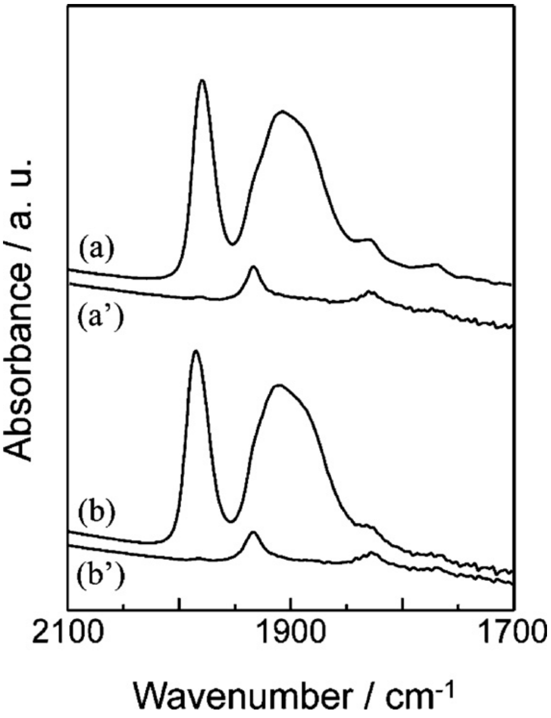

Fig. 2. FT-IR spectra of samples after evacuation at (a and b) 473 K and (a' and b') 573 K for 1 h (Samples: (a and a') HMM-phCr$(CO)_3$ and (b and b') HMM-phMo$(CO)_3$).

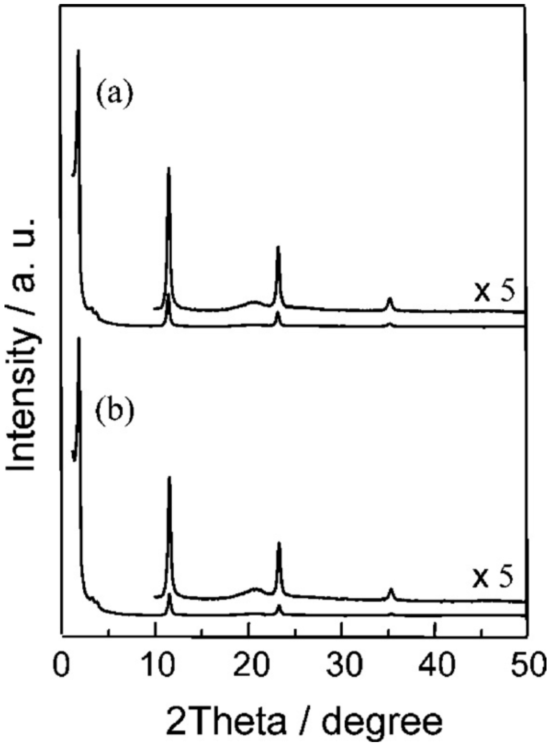

Fig. 3. XRD patterns of (a) HMM-ph and (b) HMM-phMo$(CO)_3$.

The mesoporous structures of HMM-ph and HMM-phMo$(CO)_3$ were also investigated by XRD measurements. As shown in Fig. 3, the diffraction peaks due to the two-dimensional hexagonal mesoporous structure and periodicity of the $SiO_{1.5}$–C_6H_4–$SiO_{1.5}$ units within the wall of the mesoporous framework were observed in the 2θ region from 1.5° to 50° [14]. A lattice constant ($a_0 = 2d_{100}/\sqrt{3}$) of the two-dimensional hexagonal structure was determined to be 51.5 Å from the position of an intense XRD peak in the region of $2\theta < 5°$. The shape and intensity of these diffraction peaks were found to be almost the same for both samples, showing that CVD treatment with $Mo(CO)_6$ scarcely affected the structure of HMM-ph. The incorporation of –phCr$(CO)_3$– complexes within HMM-ph was also achieved without destruction of HMM-ph (data not shown), as reported in previous literature [21,22]. The surface areas of HMM-ph, HMM-phCr$(CO)_3$ and HMM-phMo$(CO)_3$ were determined to be 806 m^2/g, 771 m^2/g and 765 m^2/g, respectively, supporting the above experimental results. Moreover, the amount of –phMe$(CO)_3$– (Me = Cr, Mo) complexes were determined to be 3.9 wt.% as Cr metal and 1.0 wt.% as Mo metal by ICP analysis for HMM-phCr$(CO)_3$ and HMM-phMo$(CO)_3$, respectively.

3.2. XAFS investigations on the local structures of –phMe(CO)$_3$– (Me = Cr, Mo) complexes

The local structure of –phCr$(CO)_3$– complexes within HMM-phCr$(CO)_3$ was investigated by XAFS measurements. The X-ray absorption near-edge structure (XANES) spectra are sensitive to the local structure and electronic state of X-ray absorbing atoms (Cr). As shown in Fig. 4, the shape of the XANES spectrum of HMM-phCr$(CO)_3$ differs from that of $Cr(CO)_6$, the CVD source of the Cr metal. The peak position of HMM-phCr$(CO)_3$ also corresponded well to that of $C_6H_6Cr(CO)_3$. As shown in Fig. 4(a), Fourier transform of the EXAFS spectrum of HMM-phCr$(CO)_3$ exhibited two peaks due

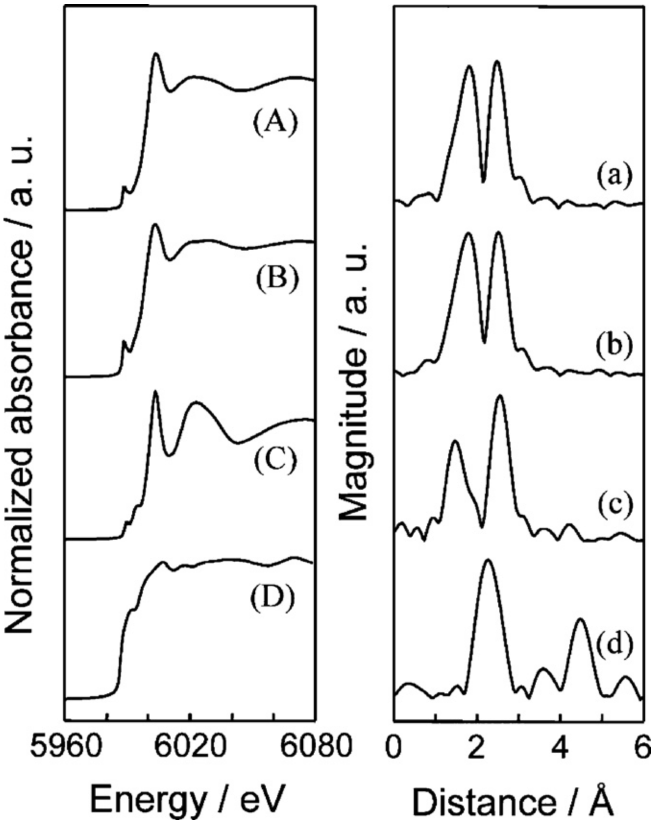

Fig. 4. (A–D) XANES and (a–d) Fourier transform of the EXAFS spectra of (A, a) HMM-phCr$(CO)_3$, (B, b) $C_6H_6Cr(CO)_3$, (C, c) $Cr(CO)_6$, and (D, d) Cr metal.

to the presence of neighboring carbon atoms (Cr–C_{ph}, Cr–C_{CO}) at around 1.8 Å and the oxygen atoms of CO (Cr–(C)O_{CO}) at around 2.5 Å (without phase-shift correction). Curve fitting analysis of the Fourier transform of EXAFS provided detailed insight into the bond distance (R) and coordination number (CN) of the –phCr$(CO)_3$– complexes. These values were determined for the Cr–C_{CO} bond (R = 1.86 Å, CN = 3.0), Cr–C_{ph} bond (R = 2.24 Å, CN = 6.0) and Cr–O_{CO} bond (R = 2.99 Å, CN = 3.0), showing good accordance with the X-ray crystallographic data of $C_6H_6Cr(CO)_3$ [31,33,34].

The local structure of the –phMo$(CO)_3$– complexes was also confirmed by XAFS measurements. Fig. 5 shows the XANES spectra of HMM-phMo$(CO)_3$ and some reference complexes of known structures. The shape of the XANES spectrum of HMM-phMo$(CO)_3$ was quite similar to that of $C_6H_6Mo(CO)_3$ as the reference complex of the arenetricarbonyl molybdenum structure. Fourier transform of the EXAFS spectra for HMM-phMo$(CO)_3$ and $C_6H_6Mo(CO)_3$ also exhibited two peaks due to the presence of neighboring carbon atoms (Mo–C_{ph}, Mo–C_{CO}) at around 1.9 Å and oxygen atoms of CO (Mo–(C)O_{CO}) at around 2.6 Å (without phase-shift correction). Curve fitting analysis of these peaks revealed the following parameters for the Mo–C_{CO} bond (R = 1.97 Å, CN = 3.0), Mo–C_{ph} bond (R = 2.38 Å, CN = 6.0) and Mo–O_{CO} bond (R = 3.11 Å, CN = 3.0), showing good coincidence with those of $C_6H_6Mo(CO)_3$ determined by X-ray crystallographic characterizations [34–36]. These results indicated that the –phMe$(CO)_3$– (Me = Cr, Mo) complexes were successfully constructed within HMM-ph without the formation of Cr and Mo metal clusters.

3.3. Polymerization of phenylacetylene on HMM-phMe$(CO)_3$ (Me = Cr, Mo)

It has been reported that arenetricarbonyl complexes exhibit catalytic activities for the polymerization of phenylacetylene (PA) in homogeneous systems [32,37,38]. Here, the same reaction was carried out on HMM-phMo$(CO)_3$ aiming at their applications for heterogeneous catalysts. During the polymerization reaction of PA, the powder color of HMM-phMo$(CO)_3$ changed from pale yellow to dark orange. Fig. 6 shows the UV–vis absorption spectra of PA and the products obtained by reprecipitation from THF after the reactions. The reaction product shows a maximum band at around 220–280 nm with a shoulder band above 300 nm, which were assigned to the π–π* transition of phenyl group and the π–π* interband transition of the polymer (polyphenylacetylene) main chain, respectively [39]. The formation of polyphenylacetylene (PPA) was also confirmed by FT-IR investigations (Fig. 7(inset)). PA shows

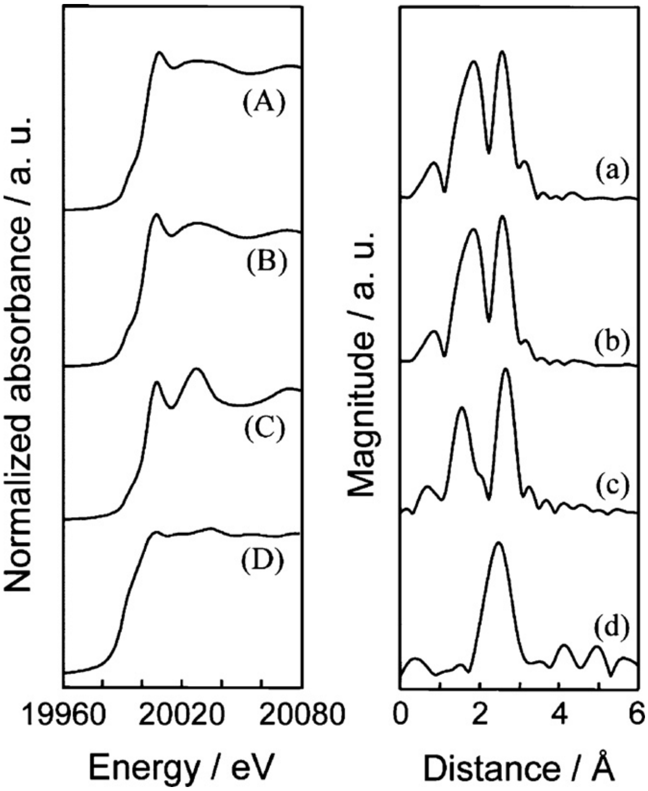

Fig. 5. (A–D) XANES and (a–d) Fourier transform of the EXAFS spectra of (A, a) HMM-phMo$(CO)_3$, (B, b) $C_6H_6Mo(CO)_3$, (C, c) $Mo(CO)_6$, and (D, d) Mo foil.

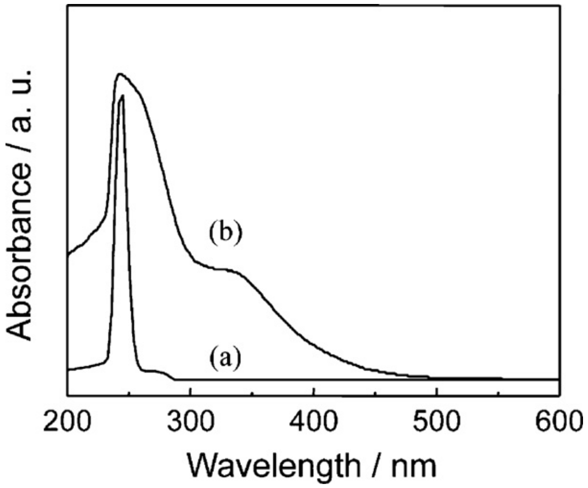

Fig. 6. UV–vis absorption spectra of (a) chloroform solution of PA and (b) chloroform solution of the obtained product by polymerization of PA on HMM-phMo$(CO)_3$.

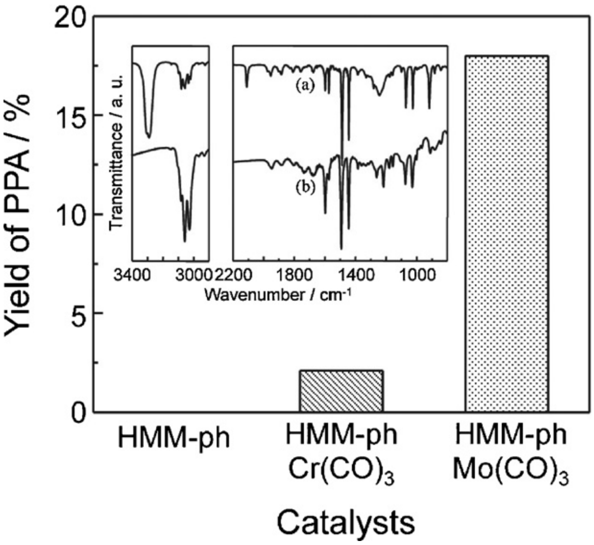

Fig. 7. Yields of polyphenylacetylene (PPA) in the polymerization reaction of PA on each catalyst. Inset shows the FT-IR spectra of (a) PA and (b) PPA produced on HMM-phMo$(CO)_3$.

typical FT-IR peaks at around 3300 and 2100 cm^{-1} due to the stretching vibration of the C–H (alkyne) and C≡C bonds, respectively, and these peaks gradually decreased during the polymerization reaction accompanied by increases in the typical FT-IR peaks of the polymerized products. The recovered reaction product shows FT-IR peaks due to the stretching vibration of the conjugated double bond at around 1600 cm^{-1} and typical C–H stretching vibration of the olefinic proton at 3020 cm^{-1} [38], which were quite different from those observed for the original PA. These results clearly indicate that the polymerization of PA proceeds on HMM-phMo$(CO)_3$ in heterogeneous systems to form PPA. The average molecular weight of the recovered PPA was ca. 8400, which was almost the same as that of PPA obtained in homogeneous systems.

Fig. 8 shows the XRD patterns of the recovered catalyst before and after washing with THF. After the polymerization reaction of PA, the peak intensities ($2\theta < 10°$) due to the two-dimensional hexagonal mesoporous structure became weak, although the peaks ($10° < 2\theta < 50°$) due to the periodicity of the $SiO_{1.5}$–C_6H_4–$SiO_{1.5}$ units scarcely changed as compared to those of the original HMM-phMo$(CO)_3$ (Fig. 3(b)). Moreover, the peak intensities ($2\theta < 10°$) of HMM-phMo$(CO)_3$, which was washed in THF after measurement (Fig. 8(a)), almost completely recovered its original intensities (Fig. 8(b)). These results suggest that the polymerization reaction of PA proceeds catalytically and PPA as a product was mainly formed within the mesopores of HMM-phMo$(CO)_3$ without the destruction of the mesoporous frameworks. Moreover, comparative studies revealed that HMM-phMo$(CO)_3$ exhibited a higher yield for the formation of PPA than HMM-phCr$(CO)_3$. As shown in Fig. 7, under the same reaction conditions, the yield of PPA was 18% on HMM-phMo$(CO)_3$ and 2.1% on HMM-phCr$(CO)_3$, respectively. Two kinds of reaction processes for the polymerization of PA have thus far been reported [32,37]. One is the metathesis reaction after the formation of an alkyl vinylidene complex. The other proceeds by way of 2 + 2 cycloaddition propagations and a ring opening reaction that follows. In both reaction processes, the coordination of PA on the metal center through the ring slipping of the η^6-arene moieties was key for the polymerization reaction. Considering that the metal–arene bond of –phCr$(CO)_3$– is stronger than that of –phMo$(CO)_3$– [32], it can be concluded that the strong phenylene–Cr metal bonding of –phCr$(CO)_3$– prevents the efficient coordination of PA to the Cr metal center, hence decreasing the reaction rate as compared to that on HMM-phMo$(CO)_3$.

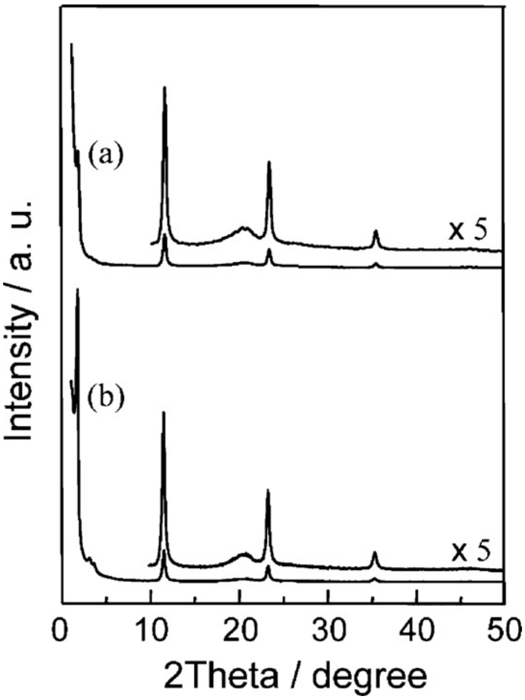

Fig. 8. XRD patterns of (a) HMM-phMo$(CO)_3$ after polymerization of PA and (b) HMM-phMo$(CO)_3$ washed in THF after measurement of (a).

Table 1
Conversion and selectivity in the dehydrochlorination of 2-chloro-2-methylbutane on HMM-ph and HMM-phMe$(CO)_3$ (Me = Cr, Mo).

Catalyst	Conversion %	Selectivity/%	
		2-Methyl-1-butene	2-Methyl-2-butene
HMM-ph	0	–	–
HMM-phCr$(CO)_3$	13.3	8.5	91.5
HMM-phMo$(CO)_3$	21.8	8.3	91.7

3.4. Dehydrochlorination reaction of 2-chloro-2-methylbutane

The dehydrochlorination of 2-chloro-2-methylbutane was carried out to investigate the catalytic performance of HMM-phMe$(CO)_3$ (Me = Cr, Mo) in the gas phase (Eq. (2)):

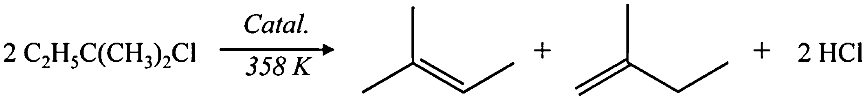

(2)

As shown in Table 1, the dehydrochlorination products, i.e., 2-methyl-1-butene and 2-methyl-2-butene were formed in this reaction system accompanied by the formation of HCl. The turnover numbers defined as the ratio of the total amount of products to the amount of –phMe$(CO)_3$– (Me = Cr, Mo) complexes were 4.8 (Cr) and 56.6 (Mo), respectively, indicating that the –phMe$(CO)_3$– complexes catalyzed dehydrochlorination even in the gas phase. In this reaction, HMM-phMo$(CO)_3$ exhibited quite higher catalytic performance than HMM-phCr$(CO)_3$. It has been reported that arenetricarbonyl chromium and molybdenum complexes act as catalysts for the dehydrochlorination reactions of organic compounds [40,41]. In these reactions, the tridentate arene ligand partially dissociates from the metal center to act as a mono- or bidentate ligand, creating coordinatively unsaturated sites which play an important role as the catalytically active sites [40,41]. The observed high catalytic performance of HMM-phMo$(CO)_3$ for the dehydrochlorination of 2-chloro-2-methylbutane can thus be ascribed to the relatively weak Mo–arene bond strength which facilitates the partial dissociation of the arene ligand from the Mo metal center.

4. Conclusions

Unique inorganic–organic hybrid mesoporous materials which incorporate arenetricarbonyl chromium and molybdenum complexes (–phMe$(CO)_3$–) within the framework of the mesopores have been successfully prepared by CVD treatment of HMM-ph with $Cr(CO)_6$ and $Mo(CO)_6$. The local structures of these complexes were investigated in detail by UV–vis, FT-IR and XAFS measurements. HMM-phMe$(CO)_3$ (Me = Cr, Mo) showed catalytic activity for the polymerization reaction of phenylacetylene as well as dehydrochlorination of 2-chloro-2-methylbutane in heterogeneous systems. Comparative studies also revealed that HMM-phMo$(CO)_3$ exhibited higher catalytic performance for both reactions than HMM-phCr$(CO)_3$ due to the relatively weak Mo–arene bond strength which facilitates the partial dissociation of the arene ligand from the Mo metal center.

Acknowledgements

The present work is supported by a Grant-in-Aid for Scientific Research (KAKENHI) from Ministry of Education, Culture, Sports, Science and Technology of Japan (No. 21550192). X-ray absorption measurements were performed at the BL-12C facility of the Photon Factory at the High-Energy Acceleration Research Organization (KEK) in Tsukuba, Japan (No. 2007G658). X-ray adsorption experiments were also performed at the BL-01B1 facility of SPring-8 at the Japan Synchrotron Radiation Research Institute (JASRI) (Nos. 2007A1669 and 2010B1530).

References

[1] A. Corma, Chem. Rev. 97 (1997) 2373.
[2] K.W. Gallis, J.T. Araujo, K.J. Duff, J.G. Moore, C.C. Landry, Adv. Mater. 11 (1999) 1452.
[3] A.P. Wight, M.E. Davis, Chem. Rev. 102 (2002) 3589.
[4] K. Moller, T. Bein, Chem. Mater. 10 (1998) 2950.
[5] V. Dufaud, F. Beauchesne, L. Bonneviot (Eds.), Angew. Chem. Int. 44 (2005) 3475.
[6] J.M. Thomas, R. Raja, D.W. Lewis (Eds.), Angew. Chem. Int. 44 (2005) 6456.
[7] M. Matsuoka, M. Anpo, J. Photochem. Photobiol. C: Photochem. Rev. 3 (2003) 225.
[8] T. Kamegawa, J. Morishima, M. Matsuoka, J.M. Thomas, M. Anpo, J. Phys. Chem. C 111 (2007) 1076.
[9] T. Kamegawa, T. Takeuchi, M. Matsuoka, M. Anpo, Catal. Today 111 (2006) 248.
[10] T. Kamegawa, N. Suzuki, M. Che, H. Yamashita, Langmuir 27 (2011) 2873.
[11] S. Inagaki, S. Guan, Y. Fukushima, T. Ohsuna, O. Terasaki, J. Am. Chem. Soc. 121 (1999) 9611.
[12] A. Stein, B.J. Melde, R.C. Schroden, Adv. Mater. 12 (2000) 1403.
[13] T. Asefa, M.J. MacLachlan, N. Coombs, G.A. Ozin, Nature 402 (1999) 867.
[14] S. Inagaki, S. Guan, T. Ohsuna, O. Terasaki, Nature 416 (2002) 304.
[15] F. Hoffmann, M. Cornelius, J. Morell, M. Fröba (Eds.), Angew. Chem. Int. 45 (2006) 3216.
[16] S. Inagaki, O. Ohtani, Y. Goto, K. Okamoto, M. Ikai, K. Yamanaka, T. Tani, T. Okada (Eds.), Angew. Chem. Int. 48 (2009) 4042.
[17] N. Mizoshita, Y. Goto, T. Tani, S. Inagaki, Adv. Mater. 21 (2009) 4798.
[18] K. Nakajima, I. Tomita, M. Hara, S. Hayashi, K. Domen, J.N. Kondo, Adv. Mater. 17 (2005) 1842.
[19] Q. Yang, J. Liu, J. Wang, M.P. Kapoor, S. Inagaki, C. Li, J. Catal. 228 (2004) 265.
[20] M. Ohashi, M.P. Kapoor, S. Inagaki, Chem. Commun. (2008) 841.
[21] T. Kamegawa, T. Sakai, M. Matsuoka, M. Anpo, J. Am. Chem. Soc. 127 (2005) 16784.
[22] M. Matsuoka, T. Kamegawa, T.H. Kim, T. Sakai, M. Anpo, J. Nanosci. Nanotechnol. 10 (2010) 314.
[23] A.C. Coelho, S.S. Balula, S.M. Bruno, J.C. Alonso, N. Bion, P. Ferreira, M. Pillinger, A.A. Valente, J. Rocha, I.S. Goncalves, Adv. Synth. Catal. 352 (2010) 1759.
[24] A.C. Coelho, S.S. Balula, M.M. Antunes, T.I. Gerganova, N. Bion, P. Ferreira, M. Pillinger, A.A. Valente, J. Rocha, I.S. Goncalves, J. Mol. Catal. A: Chem. 332 (2010) 13.
[25] E.P. Kündig, C.-H. Fabritius, G. Grossheimann, P. Romanens, Organometallics 23 (2004) 3741.
[26] H. Sun, Z. Chen, X. Zhou, Inorg. Chim. Acta 355 (2003) 404.
[27] C.J. Breheny, J.M. Kelly, C. Long, S. O'Keeffe, M.T. Pryce, G. Russell, M.M. Walsh, Organometallics 17 (1998) 3690.
[28] G. Hunter, C.H. Rochester, A.G. Wilkinson, J. Paton, J. Chem. Soc., Faraday Trans. 92 (1996) 5093.
[29] Y. Hung, R.R. Poissant, Langmuir 18 (2002) 5487.
[30] R.S. Armstrong, M.J. Aroney, C.M. Barnes, K.W. Nugent, J. Mol. Struct. 323 (1994) 15.
[31] R.S. Armstrong, M.J. Aroney, C.M. Barnes, J.A. Klepetko, T. Maschmeyer, A.F. Masters, D. Niles, J. Mol. Struct. 406 (1997) 219.
[32] T.A. Vijayaraj, G. Sundararajan, J. Mol. Catal. A: Chem. 99 (1995) 47.
[33] A. Whitaker, J.W. Jeffery, Acta Cryst. 23 (1967) 977.
[34] H.B. Bürgi, A. Raselli, D. Braga, F. Grepioni, Acta Cryst. B48 (1992) 428.
[35] J.M. Oh, S.J. Geib, N.J. Cooper, Acta Cryst. C54 (1998) 581.
[36] K. Asakura, Y. Noguchi, Y. Iwasawa, J. Phys. Chem. B 103 (1999) 1051.
[37] P.S. Woon, M.F. Farona (Eds.), J. Polym. Sci., Polym. Chem. 12 (1974) 1749.
[38] H.C.M. Vosloo, J.A.K. du Plessis, Polym. Bull. 30 (1993) 273.
[39] G. Yu, Y. Liu, X. Zhan, H. Li, M. Yang, D. Zhu, Thin Solid Films 363 (2000) 126.
[40] C.P. Tsonis, J.S. Hwang, J. Mol. Catal. 26 (1984) 219.
[41] C.P. Tsonis, M.U. Hasan, Polymer 24 (1983) 707.